tion represents strong evidence for a distinctive evolutionary origin of dinoflagellate chloroplasts, although a comparison of their plastid rRNA sequences with those of extant organisms will be required to fully resolve the issues raised here. However, it is clear that the dinoflagellate RuBisCO represents a form of the enzyme not previously found in chloroplasts.

REFERENCES AND NOTES

1. N.-E. Assali, W. F. Martin, C. C. Sommerville, S. Loiseaux-de Goër, *Plant Mol. Biol.* **17**, 853 (1991); C. W. Morden and S. S. Golden, *J. Mol. Evol.* **32**, 379 (1991); W. Martin, C. C. Somerville, S. Loiseaux-de Goër, *ibid.* **35**, 385 (1992); C. W. Morden, C. F. Delwiche, M. Kuhsel, J. D. Palmer, *BioSystems* **28**, 75 (1992).
2. F. Narang, L. McIntosh, C. Somerville, *Mol. Gen. Genet.* **193**, 220 (1984); G. Gibson and F. Tabita, *J. Biol. Chem.* **252**, 943 (1977); I. Andersson *et al.*, *Nature* **337**, 229 (1989).
3. D. Morse, unpublished data.
4. A Perkin-Elmer model 9600 PCR was run for 35 cycles of 1 min each at 95°C, 45°C, and 72°C [M. Innis, D. Gelfand, J. Sninsky, T. White, *PCR Protocols* (Academic Press, San Diego, CA, 1990)].
5. The oligonucleotides synthesized corresponded to the peptides ANITA (5′-GCNAAYATHACNGCNGAYGA-3′) and GGGAF (5′-TGNCCRAANGCNCCNCCNCC-3′) (*18*).
6. S. Machabée, L. Wall, D. Morse, *Plant Mol. Biol.* **25**, 23 (1994). The cDNAs were synthesized from poly(A) RNA and cloned into lambda ZAP vector (Stratagene, San Diego, CA). Total genomic DNA was purified by centrifugation on CsCl gradients after extraction.
7. G. Coruzzi, R. Broglie, A. Cashmore, N.-H. Chua, *J. Biol. Chem.* **258**, 1399 (1983).
8. I. Kanevski and P. Maliga, *Proc. Natl. Acad. Sci. U.S.A.* **91**, 1969 (1994).
9. P. H. Raven, *Science* **169**, 641 (1970).
10. A. I. Loeblich, *J. Protozool.* **23**, 13 (1976).
11. M. Watanabe *et al.*, *J. Phycol.* **23**, 382 (1987); L. W. Wilcox and G. J. Wedermayer, *Science* **227**, 192 (1985).
12. K. Tangen and T. Björnland, *J. Plankton Res.* **3**, 389 (1981).
13. K. Ritland and M. Clegg, *Am. Nat.* **130**, S74 (1987).
14. C. Woese, *Microbiol. Rev.* **51**, 221 (1987).
15. T. Cavalier-Smith, *Biol. J. Linn. Soc.* **17**, 289 (1982); C. Morden, C. Delwiche, M. Kuhsel, J. Palmer, *BioSystems* **28**, 75 (1992); M. W. Gray, *Trends Genet.* **5**, 294 (1989).
16. D. Yang, Y. Oyaizu, H. Oyaizu, G. J. Olsen, C. R. Woese, *Proc. Natl. Acad. Sci. U.S.A.* **82**, 4443 (1985); M. W. Gray, *Annu. Rev. Cell. Biol.* **5**, 25 (1989).
17. The extant proteobacteria *Rhodopseudomonas sphaeroides* has both form I and form II RuBisCO.
18. Abbreviations for the amino acid residues are as follows: A, Ala; C, Cys; D, Asp; E, Glu; F, Phe; G, Gly; H, His; I, Ile; K, Lys; L, Leu; M, Met; N, Asn; P, Pro; Q, Gln; R, Arg; S, Ser; T, Thr; V, Val; W, Trp; and Y, Tyr.
19. A protein extract from *Gonyaulax* cells (~1 mg of protein) was electrophoresed on two-dimensional gels [P. Milos, D. Morse, J. W. Hastings, *Naturwissenschaften* **77**, 87 (1990)].
20. The nitrocellulose membrane was stained with Ponceau red, and one 55-kD isoform was excised for microsequencing. Trypsin proteolytic fragments were sequenced by the Harvard Microchemistry Facility.
21. The gels were transferred to nitrocellulose [A. H. Towbin, T. Staehelin, J. Gordon, *Proc. Natl. Acad. Sci. U.S.A.* **76**, 4350 (1979)] and stained first with an antibody to *Rhodospirillum* RuBisCO and then with ^{125}I-labeled protein A before exposure to x-ray film. No reaction was observed with an antibody to *Nicotiana* RuBisCO used as a control.
22. DNA extracted from chloroplasts purified on Percoll gradients was purified on CsCl gradients as described [M. Schuler and R. Zielinski, *Methods in Plant Molecular Biology* (Academic Press, San Diego, CA, 1989)]. Chloroplasts were the only bodies present in the chloroplast fractions that were stained by 4′,6′-diamidino-2-phenylindole (a fluorescent DNA stain).
23. After transfer to Genescreen membranes, the samples were hybridized for 4 hours, according to the phosphate-SDS protocol of G. M. Church and W. Gilbert [*Proc. Natl. Acad. Sci. U.S.A.* **81**, 1991 (1984)], and probed with a labeled PCR fragment (oligolabeling kit from Pharmacia).
24. F. M. Ausubel *et al.*, *Current Protocols in Molecular Biology* (Green and Wiley-Interscience, New York, 1987). The filter was hybridized first to the *atpB* probe, stripped, and then hybridized to the RuBisCO probe. Both probes were exposed to x-ray film overnight.
25. The protein sequences (accession numbers: *Anabaena*, P00879; *Chromatium*, P22849; *Rhodospirillum*, P00418; *Nicotiana*, P00876; and *Gonyaulax*, L41063) were aligned with the Geneworks software package (Intelligenetics, Mountain View, CA).
26. About 100 ml of each cell culture (~1 mg of protein) was centrifuged, and then the protein was extracted from the cell pellet by sonication and heating for 10 min in two volumes of sample buffer [U. K. Laemmli, *Nature* **227**, 680 (1970)]. Equal amounts of the extracts were subjected to SDS–polyacrylamide gel electrophoresis (SDS-PAGE), and the gel was either stained with Coomassie blue or transfered to nitrocellulose. Dinoflagellates were obtained from the Bigelow laboratories, Booth Bay Harbor, MN (*G. polyedra*); Ward Scientific, St. Catharines, Ontario (*A. pacificum*); and the North East Pacific Culture Collection, Vancouver, BC (*P. lunula* and *G. aureolum*). *Nicotiana tobaccum* samples were obtained from greenhouse-grown plants at the University of Montreal.

27. We thank D. Beebe, C. Cavanaugh, W. Doolittle, S. Gibbs, and G. Lorimer for their comments on the manuscript before submission. We are grateful to G. Lorimer for making available both an antibody to proteobacteria RuBisCO and a genomic *Rhodospirillum* DNA clone, to C. Cavanaugh for providing an antibody to *Nicotiana* RuBisCO, and to F. Lang for the *atpB* gene probe. This work has been supported by a grant from the National Sciences and Engineering Research Council of Canada (D.M.), by Office of Naval Research grant N0014-94-1-0575, and by NIH grant 2R01-GM-19536 (J.W.H.).

16 September 1994; accepted 30 March 1995

Presynaptic Component of Long-Term Potentiation Visualized at Individual Hippocampal Synapses

Antonio Malgaroli,* Anthony E. Ting, Beverly Wendland, Andrea Bergamaschi, Antonello Villa, Richard W. Tsien, Richard H. Scheller

Long-term potentiation has previously been studied with electrophysiological techniques that do not readily separate presynaptic and postsynaptic contributions. Changes in exocytotic-endocytotic cycling have now been monitored at synapses between cultured rat hippocampal neurons by measuring the differential uptake of antibodies that recognize the intraluminal domain of the synaptic vesicle protein synaptotagmin. Vesicular cycling increased markedly during glutamate-induced long-term potentiation. The degree of potentiation was heterogeneous, appearing greater at synapses at which the initial extent of vesicular turnover was low. Thus, changes in presynaptic activity were visualized directly and the spatial distribution of potentiation could be determined at the level of single synaptic boutons.

The distinction between presynaptic and postsynaptic aspects of neurotransmission is fundamental to understanding how synaptic function is modulated, yet it is often difficult to assess (*1*). Vesicular release of neurotransmitter from presynaptic terminals is generally measured by electrophysiological recordings of postsynaptic signals (*2*). However, the variable responsiveness of the postsynaptic membrane renders it an unreliable indicator of presynaptic activity (*1*). This unreliability has given rise to ambiguity and controversy, particularly in the area of long-term potentiation (LTP) (*3*), for which the existence of a presynaptic component of enhancement is still intensely debated (*4*–*6*). Thus, alternative approaches are required to monitor changes in presynaptic activity directly. We now describe experiments in which vesicular fusion and recycling (*7*) were detected by the uptake of specific antibodies that recognize a luminal epitope of the vesicular protein synaptotagmin (*8*, *9*). Levels of activity during two sequential experimental periods were monitored separately with the use of two different antibody preparations, generated in different animal species, and were assessed by indirect immunofluorescence. This approach provided a ratiometric measure of changes

A. Malgaroli and A. Bergamaschi, Dibit, Scientific Institute San Raffaele, 20132 Milan, Italy.
A. E. Ting, B. Wendland, R. H. Scheller, Howard Hughes Medical Institute, Department of Molecular and Cellular Physiology, Stanford University Medical School, Stanford, CA 94305, USA.
A. Villa, Dibit, Scientific Institute San Raffaele, 20132 Milan, Italy, and Dipartimo Di Farmacologia, Universita Degli Studi Di Milano, 20132 Milan, Italy.
R. W. Tsien, Department of Molecular and Cellular Physiology, Stanford University Medical School, Stanford, CA 94305, USA.

*To whom correspondence should be addressed.

in exocytotic activity after experimental interventions and allowed each synapse to serve as its own control. Thus, synaptic modulation could be studied with great spatial resolution. We used this approach to test the idea that presynaptic modifications contribute to glutamate-induced LTP of synaptic transmission in CA3-CA1 hippocampal cultures (*5*). This form of potentiation is mediated by *N*-methyl-D-aspartate (NMDA) receptors and is strongly suppressed by postsynaptic hyperpolarization (*5*), similar to classical LTP in hippocampal slices (*3*); the potentiation can be studied in the absence of spike activity in the neuronal network (*10*).

Goat and rabbit antibodies were generated against a 24–amino acid peptide corresponding to a portion of the intraluminal domain of synaptotagmin (*11*). Immunoblot analysis of hippocampal membranes with the affinity-purified antibodies revealed a single band of 65 kD, corresponding to the mobility of synaptotagmin (Fig. 1A) (*12*). Preabsorption of either the goat or the rabbit antibodies with the synaptotagmin peptide completely abolished their ability to label the 65-kD band, confirming their specificity (Fig. 1A). To test whether the antibodies were competent for antigen binding and uptake by synaptic terminals during cycles of spontaneous synaptic vesicle turnover, we used cultured CA3-CA1 hippocampal neurons that had been obtained from 3- to 5-day-old rats and maintained in culture for 10 to 20 days (*13*). At this stage, the cultured hippocampal neurons have developed functionally mature synaptic contacts and, in response to application of glutamate, they display a long-lasting, NMDA receptor–dependent LTP of evoked and spontaneous transmission (*5*). Cultured hippocampal CA3-CA1 neurons were incubated with either the goat or rabbit antibodies to synaptotagmin (anti-synaptotagmin) in the presence of 1 μM tetrodotoxin (TTX) for 10 min to 10 hours (*14*). Neurons were then fixed and processed for immunocytochemistry (8, 9). The goat and rabbit antibodies were independently detected with fluorescently tagged, species-specific antibodies to immunoglobulin in order to identify sites of uptake (*15*). Both the rabbit and goat antibodies were efficiently internalized by hippocampal neurons (Fig. 1, B and C). The resulting punctate staining pattern corresponds to the distribution of synapses, as revealed by the precise colocalization of anti-synaptotagmin with other presynaptic terminal markers (synapsin I and synaptophysin). No staining was observed when the same experimental procedures were repeated with antibodies that recognize the cytosolic portion of synaptotagmin. Thus, staining resulted from a specific interaction of antibodies with a luminal epitope, not from a general uptake of antibodies into the cell (8, 9). A large variation was apparent in the staining intensity of individual terminals (Fig. 1, B and C). We investigated the possibility that the variation in staining correlated with the amount of synaptotagmin in the terminal. Hippocampal cultures were incubated for 1 hour with rabbit antibodies, fixed, permeabilized, and allowed to interact with goat antibodies as a measure of total synaptotagmin content. The variability persisted when corrections were made for the total synaptotagmin content of each bouton (*16*), as expected from the intrinsic variability of activity at central synapses (*17*).

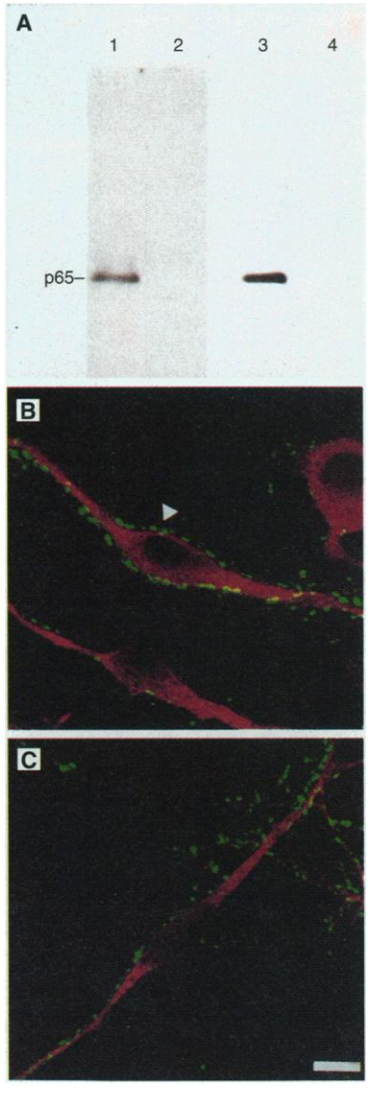

Fig. 1. Specificity and synaptic uptake of antibodies to synaptotagmin (anti-synaptotagmin). (**A**) Immunoblot analysis of rat hippocampal membranes with anti-synaptotagmin prepared in goat (lanes 1 and 2) or rabbit (lanes 3 and 4) and detected with ^{125}I-labeled protein G or ^{125}I–protein A, respectively. Preabsorption of antibodies with the immunogenic peptide completely abolished specific labeling (lanes 2 and 4). The background is higher in lanes 1 and 2 because of a fourfold longer film exposure. p65, 65-kD immunoreactive band. (**B** and **C**) Confocal microscopy of active synapses visualized by the uptake of anti-synaptotagmin generated in rabbit (B) or goat (C). Hippocampal neurons were incubated overnight in culture medium (37°C, 5% CO_2) containing antibodies and 1 μM TTX. Neurons were then fixed and processed for double-label immunostaining with mouse antibodies to microtubule-associated protein–2 (MAP-2) as counterstain and specific fluorescent secondary antibodies. The red fluorescence indicates the dendritic and somatic localization of MAP-2, and the green points represent active synaptic terminals (as judged by their precise colocalization with other synaptic markers such as synapsin I). Arrowhead, a presynaptic axon with several consecutive boutons along the same postsynaptic MAP-2–labeled dendrite. Variability in the extent of synaptic staining was apparent under control conditions, with a coefficient of variation (SD/mean) of 0.58 (rabbit) or 0.56 (goat). Bar, 25 μm.

To investigate possible variations in synaptic vesicle turnover during the course of an experiment, we incubated hippocampal cultures first with goat antibodies for 1 hour (P1) and then with rabbit antibodies for 1 hour (P2). Comparison of the relative amounts of antibody uptake during the successive incubations provided a means for visualizing changes in synaptic activity. The amount of each species of antibody internalized during P1 and P2 was quantified with the aid of a confocal fluorescence microscope system (*18*) and expressed in arbitrary units of fluorescence intensity at individual sites (F1, F2). Under control conditions, in which no experimental intervention was applied, synaptic uptake of antibodies remained relatively constant, as indicated by the similarity between the pattern and extent of the F1 and F2 signals. The ratio F2/F1 was determined for 301 individual synapses and averaged 0.88 ± 0.048 (± SEM), indicating similar uptake and detection of rabbit and goat anti-synaptotagmin. No significant differences were observed when the order of the incubations with goat and rabbit antibodies was reversed. To check that antibody application did not affect synaptic activity, we obtained whole-cell recordings from individual hippocampal neurons (Fig. 2A) (*19*). Application of the purified antibodies had no detectable effect on the frequency of miniature excitatory postsynaptic currents (EPSCs), either under control or enhanced-release conditions [average ratio relative to control, 0.98 ± 0.033 (n = 12)].

To test the ability of this approach to detect changes in synaptic activity, we examined the effect of promoting Ca^{2+} entry and thereby increasing synaptic vesicle turnover. After incubation under control conditions during P1, Ca^{2+} influx was augmented during P2 by increasing the

external K^+ concentration from 5 to 15 mM and by application of FPL 64176, a potent agonist of L-type Ca^{2+} channels (*20*). In parallel experiments with recording under whole-cell voltage clamp, this form of stimulation markedly increased the frequency of miniature EPSCs (3.6 ± 0.2–fold relative to control, $n = 15$) (Fig. 2A). The combination of increased K^+ plus FPL 64176 also enhanced the uptake of anti-synaptotagmin. Synapses that showed little staining during P1 (Fig. 2B) took up a larger number of antibodies during P2, resulting in a brightly fluorescent F2 signal (Fig. 2C). The F2/F1 ratio was determined for individual synapses and averaged 2.99 ± 0.16 ($n = 210$ synapses), more than twofold greater than control ($P < 0.0001$, t test) (Fig. 2F).

When the same intervention (15 mM K^+ and FPL 64176) was applied during P1 as well as P2, synaptic uptake was augmented during both periods, as shown by bright staining for both goat (Fig. 2D) and rabbit (Fig. 2E) antibodies; the F2/F1 ratio (1.07 ± 0.045, $n = 161$) remained close to control values. Whereas the F1 signal was affected by extending the intervention to P1, the F2 signal was not (Fig. 2G). Synaptic uptake of antibodies during P2 was not significantly affected by increased uptake during P1 ($P > 0.1$, t test) (Fig. 2G, inset) and the cumulative distributions of F2 were approximately the same (Fig. 2G). Thus, previously internalized antibodies did not affect subsequent uptake of antibody molecules or their detection with secondary antibodies.

Similar procedures were used to examine presynaptic correlates of a long-lasting synaptic potentiation elicited by a brief application of 50 μM glutamate in a Mg^{2+}-free solution (*21*). This protocol results in a clear NMDA receptor–dependent LTP in this system (*5*) and in hippocampal slices (*22*). Each preparation of cultured hippocampal cells was subjected to electrophysiological recording to verify its competence for this form of potentiation before testing it for possible changes in presynaptic vesicular turnover. Neurons were exposed for 1 hour to goat anti-synaptotagmin during P1, briefly washed, and then challenged for 30 s with either Tyrode's solution (control) or a Mg^{2+}-free solution containing 50 μM glutamate. A 1-hour exposure to rabbit antibodies (P2) was begun 10 min after the induction protocol, in order to avoid measuring short-lasting changes in activity that precede LTP (*3*). Synaptic uptake of antibodies at individual synaptic terminals was then determined. The fluorescence resulting from antibody uptake during P2 was not markedly different from that during P1 in the control experiments with mock stimulation (Fig. 3, A and B) or when the Mg^{2+}-free glutamate stimulus was applied in the presence of blockers of NMDA receptor channels [25 μM D,L-2-amino-5-phosphonovaleric acid (APV) plus 10 μM MK801]. In contrast, after the LTP induction protocol, F2 was greater than F1 (Fig. 3, C and D). The increase in F2 intensity was a consistent observation in numerous neuronal cultures ($n = 21$).

Under the specific conditions that produce LTP, the cumulative distribution of F2/F1 ratio values measured at individual synapses was markedly displaced toward higher values of F2/F1 (Fig. 3E). This shift was attributable to an enhancement of F2, indicative of increased synaptic exocytotic-endocytotic cycling during P2 (Fig. 3E, inset). The increase in ratio values relative to control was completely pre-

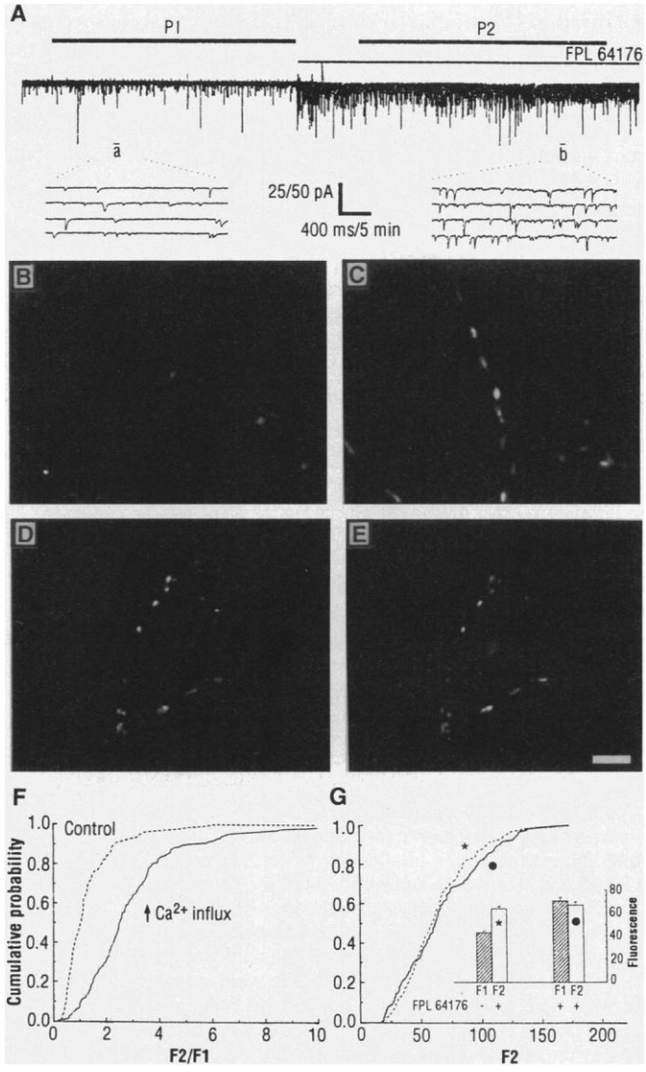

Fig. 2. Ratiometric measurement of changes in vesicular turnover associated with increased Ca^{2+} influx. (**A**) Representative example of whole-cell current recording of spontaneous EPSCs (membrane potential, −70 mV). Individual EPSCs, detected by computer analysis of digitized records (*5*), are denoted by a vertical line indicating the measured EPSC amplitude. Lower current traces are displayed on an expanded time scale. Purified anti-synaptotagmin was applied for 1 hour both under control conditions (P1, goat antibodies) and during enhanced exocytosis (P2, rabbit antibodies). Vesicular release was enhanced by application of Tyrode's solution containing 2 μM FPL 64176 and 15 mM KCl to promote Ca^{2+} influx through voltage-dependent L-type Ca^{2+} channels. FPL 64176 induced a sustained increase in miniature EPSC frequency, whereas antibodies had no effect on the frequency of spontaneous EPSCs. (**B** to **E**) Antibody internalization visualized by the sequential exposure of cultured hippocampal neurons to goat and rabbit anti-synaptotagmin, fixation, and detection with fluorescently tagged, species-specific secondary antibodies [fluorescein-labeled antibodies to goat immunoglobulin (B and D) or rhodamine-labeled antibodies to rabbit immunoglobulin (C and E)]. Bar, 8 μm (B and C) or 15 μm (D and E). (B and C) Exposure to Tyrode's solution (P1) followed by Tyrode's solution containing 15 mM K^+ plus FPL 64176 (P2), as in (A). (D and E) Two sequential exposures to Tyrode's solution containing 15 mM K^+ and FPL 64176. Note the large enhancement of synaptic staining in (C) compared to (B), and the similarity in the degree of synaptic staining in (D) and (E). (**F**) Cumulative distributions of F2/F1 values for individual synapses. Control, basal Tyrode's solution in P1 and P2 (mean F2/F1 value, 1.3 ± 0.09). ↑ Ca^{2+} influx, basal Tyrode's solution in P1, Tyrode's solution containing 15 mM K^+ and FPL 64176 in P2 (mean F2/F1 value, 2.99 ± 0.16). (**G**) Cumulative distributions of F2 values from the same sets of synapses as in the inset. (**Inset**) Pooled values of fluorescence (mean ± SEM). Left, basal Tyrode's solution in P1, Tyrode's solution containing 15 mM K^+ and FPL 64176; right, Tyrode's solution containing 15 mM K^+ and FPL 64176 in P1 and P2. Uptake of antibodies during P2 was unaffected by the degree of prior antibody internalization during P1. Likewise, retention of antibodies internalized during P1 was not altered by the degree of antibody uptake during P2. Similar results were obtained when goat and rabbit antibodies were applied in reverse order.

vented when glutamate was applied in the presence of NMDA receptor blockers, consistent with the requirement for NMDA receptors in the induction of LTP (*23*). The near twofold change in antibody uptake is comparable to the enhancement of spontaneous quantal frequency described previously (*5*).

Our approach allowed us to examine the degree of potentiation at individual synaptic terminals and to ask whether it varied systematically with synaptic behavior before potentiation (*24*). In the absence of a potentiating stimulus, there was a strong positive correlation between F2 and F1 ($r = 0.5$, $P < 0.0001$), as expected if a synapse that was more active during P1 continued to exhibit greater vesicular turnover during P2. Such a correlation was not detected in experiments in which the glutamate stimulus was applied to trigger LTP. In this instance, the synapses with an initially larger F1 tended to undergo a lesser degree of potentiation (Fig. 3, A to D). This effect is illustrated by comparison of the behavior of the overall synaptic population with that of subgroups of synapses divided according to their F1 value (Fig. 4A). The shift in the F2 distribution associated with LTP was much more pronounced for synapses with an F1 value of ≤50, and was markedly diminished for synapses with an F1 value of >50. This relation was further detailed by classifying synapses according to their F1 values and calculating the average percentage potentiation relative to control for each class (Fig. 4B). A strong negative correlation between F1 and the degree of potentiation was evident. The same correlation was apparent for large and small boutons (*25*). The variability in F1 values persisted after correction for the amount of total synaptotagmin immunoreactivity in individual boutons, indicating a genuine variation in the level of exocytotic-endocytotic activity during the control period (*16*). Synapses with initially low synaptic activity might be expected to exhibit a greater capacity to undergo potentiation relative to synapses with high initial activity (*26*). Our data support the idea that this capability can be realized under the influence of a strongly potentiating stimulus.

Thus, we have visualized directly an enhancement of presynaptic activity in association with long-lasting glutamate-induced potentiation of spontaneous transmission at hippocampal synapses. Such potentiation is known to be paralleled by a persistent increase in evoked transmission and is prevented by NMDA receptor blockers or postsynaptic hyperpolarization (*5*), as is LTP in hippocampal slices (*3*, *23*). The ratiometric measurements of antibody uptake allowed us to monitor changes in presynaptic vesicular turnover directly. This approach bypasses postsynaptic receptors as indicators and thus provides information distinct from that obtained in electrical recordings. An advantage of the present method is its ability to detect changes at the single-bouton level, which offers a way of analyzing synaptic plasticity against a background of great variability within a large population of synapses (*17*). Indeed, the degree of potentiation was highly heterogeneous, varying inversely with the initial level of antibody uptake at individual nerve terminals, as if synapses with low or high basal activity approach a common ceiling after potentiation (*27*). The spatial resolving power of our antibody method may be valuable for studying the spread of LTP among neighboring synapses (*28*) and in the mapping of patterns of stably expressed potentiation in complex neural networks.

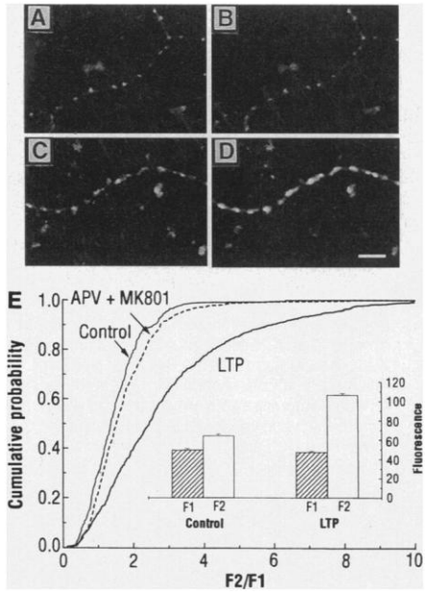

Fig. 3. Visualization of the enhancement of vesicular turnover at individual boutons. (**A** and **B**) Hippocampal neurons were subjected to a mock application of control solution after P1, followed 10 min later by P2. Indirect immunofluorescence reflects the spatial distribution of goat antibodies taken up during P1 (A) and rabbit antibodies taken up during P2 (B). All incubations with antibodies were performed in the constant presence of APV (25 μM) to avoid possible potentiation by intrinsic spontaneous activity. (**C** and **D**) Hippocampal neurons were subjected after P1 to an LTP-inducing stimulus, consisting of a brief (5 s) wash with a Mg^{2+}-free solution followed by a 30-s challenge with Mg^{2+}-free solution containing 50 μM glutamate (*5*). P2 began 10 min after the end of the induction protocol. The spatial distributions of goat antibodies taken up during P1 (C) and rabbit antibodies taken up during P2 (D) are shown. Antibody uptake during P2 was greatly increased relative to that observed in control experiments (B). Bar, 10 μm. (**E**) Cumulative probability distributions of F2/F1 values for individual synapses. Control, sham application of control solution in place of the LTP-inducing stimulus ($n = 377$ synapses); LTP, 30-s glutamate application ($n = 843$ synapses); APV + MK801, the glutamate challenge was performed in the presence of the NMDA receptor blockers APV (25 μM) and MK801 (10 μM) ($n = 387$ synapses). The distributions were obtained from three individual experiments in which the synaptic signal-to-background ratio was very high, thus allowing a precise estimation of basal and potentiated synaptic uptake of antibodies. The mean F2/F1 ratio was 1.48 ± 0.04 in control, 2.93 ± 0.07 with the LTP induction procedure, and 1.76 ± 0.05 with the induction procedure performed in the presence of APV and MK801. (**Inset**) Mean values of F1 and F2 for experiments with the sham application (control) and LTP induction procedure (LTP). Whereas F2 was significantly greater after the LTP procedure, thus explaining the increased F2/F1 ratio, F1 values were not significantly different between control and LTP induction. These observations indicate that there is no detectable loss of internalized antibodies as a consequence of the increased level of exocytotic-endocytotic cycling associated with induction of LTP.

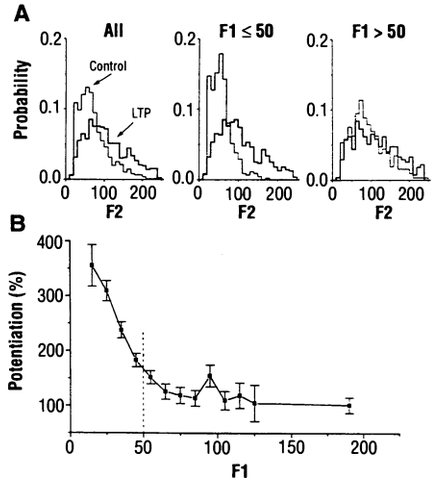

Fig. 4. Correlation of synaptic enhancement with the basal level of synaptic activity. (**A**) Distributions of F2 values in control and LTP-induction procedures for the overall synaptic population (all) and for subpopulations sorted by their F1 values (F1 ≤ 50, F1 > 50). The difference in F2 values between control and LTP was more pronounced in boutons in which F1 values were initially low and was almost absent when F1 values were high. Same data set as presented in Fig. 3E. Quantitation of the pixel intensities for synapses shown in Fig. 3, A to D, gave results consistent with the overall trend. (**B**) Mean percentage potentiation for subgroups of synapses, binned according to their F1 values after subtraction of corresponding control values, calculated as $\{[(F2/F1)_{LTP}/(F2/F1)_{con}] - 1\}$ multiplied by 100%. Bars are SEMs calculated according to the formula, variance = variance_{LTP} + variance_{con}. The dashed line indicates F1 = 50, the cutoff value used to sort synapses (A).

REFERENCES AND NOTES

1. F. Edwards, *Nature* **350**, 271 (1991); C. F. Stevens, *Cell* **72**, 55 (1993).
2. J. del Castillo and B. Katz, *J. Physiol. (London)* **124**, 560 (1954); A. Lev-Tov and R. Rahamimoff, *ibid.* **309**, 247 (1980).
3. T. V. P. Bliss and G. L. Collingridge, *Nature* **361**, 31 (1993).
4. M. A. Lynch and T. V. P. Bliss, *Brain Res.* **369**, 405 (1986); R. Malinow and R. W. Tsien, *Nature* **346**, 177 (1990); J. M. Bekkers and C. F. Stevens, *ibid.*, p. 724; D. M. Kullmann and R. A. Nicoll, *ibid.* **357**, 240 (1992); D. Liao, A. Jones, R. Malinow, *Neuron* **9**, 1089 (1992).
5. A. Malgaroli and R. W. Tsien, *Nature* **357**, 134 (1992).
6. T. C. Foster and B. L. McNaughton, *Hippocampus* **1**, 79 (1991); T. Manabe, P. Renner, R. A. Nicoll, *Nature* **355**, 50 (1992); T. Manabe and R. A. Nicoll, *Science* **265**, 1888 (1994).
7. J. Meldolesi and B. Ceccarelli, *Curr. Top. Membr. Transp.* **32**, 139 (1988); M. Matteoli and P. De Camilli, *Curr. Opin. Neurobiol.* **1**, 91 (1991); W. J. Betz and G. S. Bewick, *Science* **255**, 200 (1992); T. A. Ryan *et al.*, *Neuron* **11**, 713 (1993); P. S. McPherson and P. De Camilli, *Semin. Neurosci.* **6**, 137 (1994).
8. M. Matteoli, K. Takei, M. S. Perin, T. C. Südhof, P. De Camilli, *J. Cell Biol.* **117**, 849 (1992).
9. L. A. Elferink, M. R. Peterson, R. H. Scheller, *Cell* **72**, 153 (1993).
10. Tetrodotoxin (TTX) was used to eliminate spike activity, as verified by direct electrical recordings. The increase in spontaneous transmitter release can be suppressed by hyperpolarization of individual postsynaptic cells during the induction maneuvers (*5*); once induced, the potentiation is well maintained, even during removal of extracellular Ca^{2+} (*5*), further indicating that it does not involve reverberatory action potential activity and depolarization-induced synaptic transmission.
11. Polyclonal antisera were obtained from rabbits and a goat immunized with a synthetic peptide (H_2N-Met-Val-Ser-Ala-Ser-His-Pro-Glu-Ala-Leu-Ala-Ala-Pro-Val-Thr-Thr-Val-Ala-Thr-Leu-Val-Pro-His-Cys-COOH) corresponding to the intravesicular NH_2-terminal portion of synaptotagmin I. Specific antibodies were purified with an affinity column prepared by cross-linking the synthetic peptide to Affi-Gel 102 beads (Bio-Rad, Hercules, CA) via sulfhydryl groups. Antiserum was incubated overnight with beads containing cross-linked peptide and the bound antibodies were eluted with 0.1 M glycine (pH 2.5). The affinity-purified antibodies were dialyzed against phosphate-buffered saline (PBS) and stored at −80°C.
12. M. S. Perin, V. A. Fried, G. A. Mignery, R. Jahn, T. Südhof, *Nature* **345**, 260 (1990).
13. Cultures of CA3-CA1 hippocampal neurons were prepared essentially as described (*5*). Briefly, the hippocampal CA3 and CA1 regions were removed from 3- to 5-day-old rats and the neurons recovered by enzymatic digestion [trypsin type XI (10 mg/ml), deoxyribonuclease I type IV (0.5 mg/ml)] and mechanical dissociation. The cells were cultured in Eagle's minimum essential medium containing 0.6% glucose, 1 mM glutamine, $NaHCO_3$ (2.4 g/liter), bovine transferrin (100 mg/ml), insulin (25 mg/ml), and 5 to 10% fetal bovine serum and were plated at a density of 50,000 per dish on petri dishes (Falcon, 30 mm) coated with polyornithine and Matrigel (Collaborative Research). Cultures were maintained at 37°C under a humidified atmosphere of 95% air and 5% CO_2. The culture medium was replaced every 3 to 4 days. From the second day in culture, the medium was supplemented with 5 μM cytosine-D-arabinofuranoside. Neurons were used for synaptic uptake experiments 10 to 20 days after plating. All chemicals were obtained from Sigma (Milan, Italy), with the exception of TTX (Latoxan, Rosans, France), transferrin (Calbiochem), MK801 (Burroughs-Wellcome, Cambridge, UK), and FPL 64176 (provided by J. W. Shipman, Fisons). Culture medium and fetal bovine serum were from Gibco (Milan, Italy).
14. In all experiments, anti-synaptotagmin was added to serum-free culture medium supplemented with 1 μM TTX at a final dilution of 1:200 (rabbit) or 1:50 (goat) and incubated with the hippocampal cultures under a humidified atmosphere of 95% air and 5% CO_2. In addition, the cultures were washed extensively with oxygenated Tyrode's solution (37°C) [119 mM NaCl, 5 mM KCl, 2 mM $CaCl_2$, 4 mM $MgCl_2$, 30 mM glucose, 1 mM glycine, 25 mM Hepes (pH 7.4)] supplemented with 25 μM APV before and between antibody incubations. The synaptic uptake of antibodies was preserved when Fab fragments (produced by papain digestion) were used.
15. For immunofluorescence studies, hippocampal neurons were grown on glass coverslips, incubated with anti-synaptotagmin, washed, and fixed (*8*). After incubation for 1 to 2 hours at room temperature in PBS containing 1% bovine serum albumin, 2% normal donkey serum, and 0.4% saponin (blocking solution), the neurons were exposed for 1 hour at room temperature to fluorescently labeled secondary antibodies diluted 1:100 in blocking solution [dichlorotriazinylamino fluorescein–conjugated donkey antibodies to goat immunoglobulin (Chemicon, Temcula, CA) and lissamine rhodamine–conjugated donkey antibodies to rabbit immunoglobulin (Jackson ImmunoResearch Laboratories, West Grove, PA)]. The cover slips were then washed three times with 100 mM glycine in PBS and mounted on glass slides in Citifluor (UKC Chemical Laboratory, Canterbury, UK). For these studies, we used fluorescent secondary antibodies that had been preabsorbed with antibodies from other species to reduce cross-reactivity. Microscopy and confocal imaging were performed with an inverted microscope (60× oil-immersion objective) and a Multiprobe 2001 laser confocal system (Molecular Dynamics). Areas of antibody staining were first identified by epifluorescence of either fluorescein or rhodamine. Synaptic boutons in these images were then identified on the basis of their pattern of fluorescence (Fig. 1, B and C), and the fluorescence intensities near the middle of individual boutons were quantitated with ImageSpace software (Molecular Dynamics). No background subtraction was performed in order to avoid overcorrection of intensity values, which might tend to give spuriously high values in ratio determinations.
16. Relative estimates of the total synaptotagmin content in individual boutons were obtained as follows. Hippocampal cultures that had been allowed to take up rabbit anti-synaptotagmin during a prior 1-hour test period were washed, fixed, and incubated in blocking solution for 1 hour. The cultures were then incubated with goat anti-synaptotagmin for 1 hour, washed, incubated with fluorescent secondary antibodies and prepared for microscopy as described (*15*). The staining with the goat antibodies provided an index of the total amount of synaptotagmin. Estimates of total synaptotagmin were used to normalize the P1 signal (see text). The resulting distribution showed a marked variability among boutons (coefficient of variation, 1.24), consistent with wide variations in the extent of vesicular turnover.
17. C. Rosenmund, J. D. Clements, G. L. Westbrook, *Science* **262**, 754 (1993); N. A. Hessler, A. M. Shirke, R. Malinow, *Nature* **366**, 569 (1993); T. H. Murphy, J. M. Baraban, W. G. Wier, L. A. Blatter, *Science* **263**, 529 (1994).
18. Hippocampal cultures were imaged with a Multiprobe 2001 laser confocal microscope system and an argon-krypton laser with excitation wavelengths at 448 and 568 nm. The fluorescence intensities of synaptic boutons were quantitated with ImageSpace software. Potential bias in the quantitation of these studies was avoided by coding of the slides by another individual after slide processing was completed. All subsequent image acquisition and quantitation steps were performed without prior knowledge of the experimental treatment. After quantitation was completed, the code was disclosed and the appropriate data were assembled for control, LTP, and NMDA receptor blocker trials (Fig. 3).
19. Whole-cell recordings were obtained at room temperature (23° to 25°C) from pyramidal cells 10 to 14 days after cell plating with an Axopatch 1-D amplifier (Axon). The input and series resistances were monitored during the course of the experiment. The bath was perfused continuously (2 ml/min) with oxygenated control Tyrode's solution (*14*) containing 2 mM $MgCl_2$ and supplemented with 0.1 mM picrotoxin and 1 μM TTX. Patch electrodes (resistance, 5 to 10 megohms) contained 102 mM cesium gluconate, 5 mM $MgCl_2$, 10 mM NaCl, 0.6 mM EGTA (Cs^+ salt), 2 mM adenosine triphosphate, 0.2 mM guanosine triphosphate, and 49 mM Hepes (pH 7.2). For experiments in which Ca^{2+} influx was promoted, Tyrode's solution was supplemented with 25 μM APV, 10 μM MK801, and 6 mM $MgCl_2$ (final concentration).
20. W. Zheng, D. Rampe, D. J. Triggle, *Mol. Pharmacol.* **40**, 734 (1991); A. Randall and R. W. Tsien, *J. Neurosci.* **15**, 2995 (1995).
21. For LTP experiments, culture medium used for antibody incubations was supplemented with 25 μM APV. Before and after antibody incubations, neurons were extensively washed with oxygenated prewarmed Tyrode's solution containing 25 μM APV and 4 mM $MgCl_2$. To induce potentiation, we briefly washed dishes with Tyrode's solution containing no added NMDA receptor blockers, followed by a 5-s wash with a $MgCl_2$-free Tyrode's solution, and then challenged the neurons for 30 s with 50 μM glutamate in $MgCl_2$-free solution. At the end of the glutamate pulse, cells were washed quickly with the Tyrode's solution lacking NMDA receptor blockers, followed by many washes with Tyrode's solution containing 25 μM APV and 4 mM $MgCl_2$. The second incubation with anti-synaptotagmin was started 10 min after the end of the glutamate pulse. To be certain of the identification of synapses, we chose not to study potentiation at sites for which either the F1 or F2 fluorescence signal fell below a preset threshold. Thus, if the synapse was silent in the first control period, it was excluded. This approach results in a conservative estimate of the degree of potentiation because recruitment of silent synapses was not considered.
22. R. C. Malenka, *Neuron* **6**, 53 (1991); R. J. Cormier, M. D. Mauk, P. T. Kelly, *ibid.* **10**, 907 (1993).
23. G. L. Collingridge, S. J. Kehl, H. McLennan, *J. Physiol. (London)* **334**, 33 (1983).
24. A. Larkman, T. Hannay, K. Stratford, J. Jack, *Nature* **360**, 70 (1992).
25. Large boutons showed a similar distribution of F1 values to that of small boutons, as might be expected because the analysis of intensity focused on pixels near the centers of boutons (*15*). Furthermore, when boutons were subdivided by size into two groups, large and small, both groups showed similar correlations between low values of F1 and stronger potentiation.
26. E. J. Coan, A. J. Irving, G. L. Collingridge, *Neurosci. Lett.* **105**, 205 (1989); X. D. Yang and D. S. Faber, *Proc. Natl. Acad. Sci. U.S.A.* **88**, 4299 (1991); Y. Huang, A. Colino, D. K. Selig, R. C. Malenka, *Science* **255**, 730 (1992); Y. Izumi, D. B. Clifford, C. F. Zorumski, *ibid.* **257**, 1273 (1992).
27. This observation may be consistent with studies of LTP in hippocampal slices, in which the relative contribution of a putative presynaptic enhancement varies inversely with the initial probability of transmitter release (*24*). The level of F2 was not constrained by a limitation of the detection system, being far below the fluorescence signal obtained with overnight antibody incubation.
28. T. Bonhoeffer, V. Staigern, A. Aertsen, *Proc. Natl. Acad. Sci. U.S.A.* **86**, 8113 (1989); E. Schuman and D. M. Madison, *Science* **263**, 532 (1994).

29. We thank J. Meldolesi, T. Pozzan, D. DiFrancesco, E. Schuman, L. Forti, E. Naldi, and J. Noel for helpful discussions; M. Bossi for technical assistance; and M. Krasnow for the use of his confocal microscope system. Supported by European Community (EC) grant BMH*-CT92-0008 (A.M.), Italian National Research Council (CNR) grant 93.01754.CT04 (A.M.), Telethon grant D16 (A.M.), and the National Institutes of Mental Health Silvio Conte Center at Stanford (R.W.T. and R.H.S.).

11 October 1994; accepted 22 March 1995